Title page

Association of sleep-disordered breathing with Alzheimer's disease biomarkers in community-dwelling older adults

A Secondary Analysis of a Randomized Clinical Trial

Claire André[1,2], PhD; Stéphane Rehel[1,2], MSc; Elizabeth Kuhn[1], MSc; Brigitte Landeau[1], MSc; Inès Moulinet[1], MSc; Edelweiss Touron[1], MSc; Valentin Ourry[2], MSc; Gwendoline Le Du[1], MSc; Florence Mézenge[1], BA; Clémence Tomadesso[1], PhD; Robin de Flores[1], PhD; Alexandre Bejanin[1], PhD; Siya Sherif[1], PhD; Nicolas Delcroix[3], PhD; Alain Manrique[4], MD, PhD; Ahmed Abbas[2], PharmD; Natalie L. Marchant[5], PhD; Antoine Lutz[6], PhD; Olga M. Klimecki[7], PhD; Fabienne Collette[8], PhD; Eider M. Arenaza-Urquijo[1], PhD; Géraldine Poisnel[1], PhD; Denis Vivien[1,9], PhD; Françoise Bertran[10], MD; Vincent de la Sayette[2,11], MD; Gaël Chételat[1]*, PhD; Géraldine Rauchs[2]*, PhD; for the Medit-Ageing Research Group.

[1] Normandie Univ, UNICAEN, INSERM, U1237, PhIND "Physiopathology and Imaging of Neurological Disorders", Institut Blood and Brain @ Caen-Normandie, Cyceron, 14000 Caen, France.

[2] Normandie Univ, UNICAEN, PSL Université, EPHE, INSERM, U1077, CHU de Caen, GIP Cyceron, NIMH, Caen, France.

[3] CNRS, UMS-3048, GIP Cyceron, Bd Henri Becquerel, Caen, France.

[4] Normandie Univ, UNICAEN, EA 4650 SEILIRM, GIP Cyceron, Caen, France.

[5] Division of Psychiatry, University College London, London, United Kingdom.

[6] Lyon Neuroscience Research Center INSERM U1028, CNRS UMR5292, Lyon University, Lyon, France.

[7] Swiss Center for Affective Sciences, Department of Medicine, University of Geneva, Geneva, Switzerland.

[8] GIGA-CRC, In Vivo Imaging and Psychology and Cognitive Neuroscience Unit, Liège University, Belgium.

[9] Département de Recherche Clinique, CHU Caen-Normandie, Caen, France.

[10] Unité d'exploration et de traitement des troubles du sommeil, CHU de Caen, Caen, France.

[11] Service de Neurologie, CHU de Caen, Caen, France.

* Equal contribution as last author.

Corresponding author:

Dr Gaël Chételat,

Inserm UMR-S U1237,

GIP Cyceron, Bd Henri Becquerel, BP 5229, 14074 Caen cedex 5, France

chetelat@cyceron.fr

Word count: 2992/3000

Date of revision: December 17, 2019.

Key points:

- **Question:** Which brain changes are associated with sleep-disordered breathing (SDB) in aging?
- **Findings:** In this cross-sectional study of 127 cognitively unimpaired community-dwelling older individuals, the presence of SDB was associated with greater amyloid burden, gray matter volume, metabolism, and perfusion in the posterior cingulate cortex and precuneus. There was no association with cognitive performance, self-reported cognitive or sleep difficulties, nor excessive daytime sleepiness.
- **Meaning:** SDB-related changes include amyloid deposition in brain regions typically involved in Alzheimer's disease (AD), which might explain why SDB is associated with an increased risk for developing Alzheimer's clinical syndrome at a younger age.

Abstract:

Importance: Increasing evidence suggests that sleep-disordered breathing (SDB) increases the risk of developing Alzheimer's clinical syndrome. However, the brain mechanisms underlying the link between SDB and Alzheimer's disease (AD) are still unclear.

Objective: To determine which brain changes are associated with the presence of SDB in cognitively unimpaired older individuals, including changes in amyloid deposition, gray matter (GM) volume, perfusion and glucose metabolism.

Design and Setting: This cross-sectional study was conducted using data from the Age-Well randomized controlled trial (RCT) of the Medit-Ageing European project, acquired between 2016 and 2018 at Cyceron Center (Caen, France).

Participants: On 157 community-dwelling older adults assessed for eligibility, 137 were enrolled in the Age-Well RCT (20 were excluded owing to medical or cognitive exclusion criteria or not willing to participate).

Main outcomes and measures: 127 participants who completed a detailed neuropsychological assessment, a polysomnography, MRI, Florbetapir-, and FDG-PET scans were included in the analyses. Based on the apnea-hypopnea index (AHI), they were classified as SDB- (AHI<15, n=31) or SDB+ (AHI≥15, n=96). Voxel-wise between-group comparisons were performed for each neuroimaging modality, and secondary analyses aimed at (i) identifying which SDB parameter (sleep fragmentation, hypoxia severity or the frequency of respiratory disturbances) best explained the observed brain changes, and (ii) assessing whether SDB severity and/or SDB-related brain changes are associated with cognitive and behavioral changes.

Results: The mean (SD) age of the 127 participants was 69.05 (3.86) years, and 80 (63%) were women. SDB+ participants showed greater amyloid burden (T=4.51; $P_{FWE\text{-}corrected}$=.04; Cohen's d=0.83), GM volume (T=4.12; $P_{FWE\text{-}corrected}$=.04; Cohen's d=0.75), perfusion

(T=4.62; $P_{FWE\text{-}corrected}$=.001; Cohen's d=0.86) and metabolism (T=4.63; $P_{FWE\text{-}corrected}$=.001; Cohen's d=1.04) overlapping mainly over the posterior cingulate cortex and precuneus. No association was found with cognition, self-reported cognitive and sleep difficulties, or excessive daytime sleepiness symptoms.

Conclusions and relevance: SDB-related brain changes in cognitively unimpaired older adults include greater amyloid deposition and neuronal activity in AD-sensitive brain regions, notably the posterior cingulate cortex and precuneus. These results support the need to screen and treat for SDB, especially in asymptomatic older populations, in order to reduce AD risk.

Manuscript text

1. Introduction

Sleep-disordered breathing (SDB) is a respiratory disorder characterized by recurrent upper airway collapse during sleep, associated with intermittent hypoxia and sleep fragmentation[1,2]. It affects 30 to 80% of cognitively unimpaired older adults, depending on SDB definition criteria[3,4]. Patients with a clinical diagnosis of Alzheimer's disease (AD) are even more likely to suffer from SDB[5], and untreated SDB is associated with cognitive decline and conversion to Alzheimer's clinical syndrome at a younger age[6–8].

In order to clarify the mechanisms underlying the association between SDB and dementia risk, growing efforts have been deployed to better characterize the brain changes associated with SDB. Yet, previous studies have provided heterogeneous results, showing both SDB-related decreases[9–11] and increases[12,13] in gray matter (GM) volume or cortical thickness in various brain areas including frontal, temporal and parietal regions. Similarly, both decreased[14–16] and increased[15,17] perfusion has been reported in SDB patients compared to controls. Finally, SDB has been related to increased amyloid and tau levels in the blood and cerebrospinal fluid (CSF), both cross-sectionally and longitudinally[18–21]. However, cross-sectional PET studies have reported inconsistent results, some showing greater amyloid burden in association with SDB[22,23], while others do not report significant associations[21,24]. These discrepancies may be explained by the characteristics of SDB patients (e.g., recruited from sleep clinics versus from the community, differences in age and disease duration), the scoring criteria of respiratory events, sample sizes, and/or the lack of control for possibly biasing covariates.

To our knowledge, no previous study has used a multimodal neuroimaging approach to highlight early brain changes associated with the presence of untreated SDB within a large

sample of cognitively unimpaired older participants recruited from the community, with no or few symptoms. Therefore, our main objective was to provide a comprehensive picture of structural, functional and molecular brain changes associated with untreated SDB in aging, in order to provide significant advances in our understanding of early brain mechanisms underlying the relationships between SDB and AD. Secondary objectives aimed at identifying which aspect of SDB severity (i.e., sleep fragmentation, hypoxia severity or the frequency of respiratory events), is most associated to brain changes. Lastly, we investigated the associations between SDB severity and/or SDB-related brain changes and cognitive performance, self-reported cognitive and sleep difficulties, or symptoms of sleepiness.

2. Materials & Methods.

2.1. Participants

We included 127 cognitively unimpaired older adults from the baseline visit of the Age-Well randomized controlled trial (RCT) of the Medit-Ageing European project[25] (flow diagram in **Figure 1**), sponsored by the French National Institute of Health and Medical Research (INSERM). Participants were recruited from the general population, aged over 65 years old, native French speakers, retired for at least one year, having completed at least 7 years of education, and performing within the normal range on standardized cognitive tests. Main exclusion criteria were safety concerns in relation to MRI or PET scanning, evidence of a major neurological or psychiatric disorder, including alcohol or drug abuse, history of cerebrovascular disease, presence of a chronic disease or acute unstable illness, and current or recent medication that may interfere with cognitive functioning.

Participants meeting inclusion criteria performed a detailed cognitive assessment, a polysomnography, structural MRI, ^{18}F-Florbetapir and ^{18}F-fluorodeoxyglucose (FDG) PET

scans and Apolipoprotein E ε4 (APOE4) genotyping within a maximum period of 3 months. All participants gave their written informed consent prior to the examinations, and the Age-Well RCT was approved by the ethics committee (CPP Nord-Ouest III, Caen; trial registration number: EudraCT: 2016- 002441-36; IDRCB: 2016-A01767-44; ClinicalTrials.gov Identifier: NCT02977819).

2.2. Cognitive and behavioral assessment

The detailed neuropsychological evaluation encompassed global cognitive functioning, processing speed, attention, working memory, executive functions, and episodic memory[25]. For each cognitive domain, a composite score was computed (see eAppendix1 in the Supplement for further details). In addition, self-reported cognitive difficulties were assessed using the Cognitive Difficulties Scale[26]. Moreover, self-reported sleep quality was assessed using the Pittsburgh Sleep Quality Index (PSQI)[27], and excessive daytime sleepiness symptoms were measured using the Epworth Sleepiness Scale (ESS)[28].

2.3. Neuroimaging examinations

All participants underwent a high-resolution T1-weighted anatomical image to measure GM volume, and a Florbetapir-PET scan, with a 10 min early acquisition, beginning immediately after the intravenous injection, reflecting brain perfusion, and a 10 min late acquisition (beginning 50 mn after injection) reflecting amyloid burden. A subset of participants (n=87) also underwent an ^{18}F-fluorodeoxyglucose (FDG)-PET scan, to measure brain glucose metabolism. All participants were scanned at Cyceron Center (Caen, France) on the same MRI (Philips Achieva 3.0T) and PET (Discovery RX VCT 64 PET-CT, General Electric Healthcare) scanners. The detailed acquisition and pre-processing procedures are available in the eAppendix1 in the Supplement (see also [25]). PET analyses were performed on images

corrected for partial volume effects (PVE) using the three-compartmental voxel-wise Müller-Gartner method[29].

2.4. SDB characterization

Participants underwent a polysomnography (PSG) using a portable home device (Siesta®, Compumedics, Australia). Acquisition parameters are described in the eAppendix1 in the Supplement. Sixty-eight percent of the participants (n=86 over 127) underwent two PSG recordings, including a habituation night which was not included in the analyses. The remaining 39 participants only had one PSG recording. Recordings were visually scored in 30-s epochs following the recommended standard criteria of the American Academy of Sleep Medicine[1]. Sleep apnea was defined by a ≥90% drop of nasal pressure for at least 10 seconds, whereas sleep hypopnea was characterized by a ≥30% drop of nasal pressure for a minimum of 10 seconds, associated with an arousal or a ≥3% oxygen desaturation.

Based on the apnea-hypopnea index (AHI) (i.e., the sum of apneas and hypopneas per hour of sleep), participants were classified into two groups with a cut-off value of 15, independently of clinical symptoms, in accordance with the recommendations of the 3rd edition of the International Classification of Sleep Disorders[30]. Thus, we obtained a SDB- group (AHI<15; n=31) and a SDB+ group (AHI≥15; n=96)[6,20,31,32]. The sub-sample of 87 participants who also had a FDG-PET scan was composed of 69 SDB+ and 18 SDB- participants, who did not differ from the main sample regarding the proportion of SDB+ versus SDB- participants (χ^2=0.26, P=.61), demographic, sleep and cognitive variables (data not shown).

Lastly, to address secondary objectives, we computed two composite scores reflecting sleep fragmentation and hypoxia severity. This composite score approach, also used in a previous study[12], was preferred to a single-item approach, in order to minimize the issue of multiple statistical testing. The sleep fragmentation composite score corresponded to the average of the

Z-scores of the respiratory arousal index, the number of shifts to non-REM sleep stage 1 per hour, and the number of nocturnal awakenings per hour. The hypoxia composite score corresponded to the average of the Z-scores of the oxygen desaturation index, the proportion of total sleep time with oxygen desaturation ≤90%, and the minimal oxygen saturation.

2.5. Statistical analyses

2.5.1. Between-group differences

Between-group differences for demographical, behavioral, sleep, and cognitive variables were assessed using Student t-tests for continuous variables, and chi-square statistics for categorical variables, with statistical significance set to P<.05.

Voxel-wise group differences in amyloid burden, GM volume, perfusion and glucose metabolism were explored using ANCOVAs in SPM12, controlling for age, sex, education, body mass index (BMI), sleep medication use, and ApoE4 status. Voxel-wise analyses were performed using MRI and PVE-corrected PET data, and considered significant at a voxel-level P<.005 (uncorrected) threshold and a cluster-level threshold of P<.05 corrected for family-wise errors (FWE).

2.5.2. Stepwise regression analyses

As a second step, we aimed at further assessing which aspect of SDB severity (i.e., the frequency of respiratory disturbances, associated sleep fragmentation and/or hypoxia severity) was more specifically involved in the SDB-related brain changes highlighted in the previous analysis. For this purpose, amyloid burden, GM volume, perfusion and glucose metabolism signal values were extracted from the significant clusters obtained in the voxel-wise group comparisons described above. Then, stepwise regression analyses were performed on the whole sample of participants with nine measures entered in the model as independent

variables (i.e., the AHI, the sleep fragmentation composite score, the hypoxia composite score, age, sex, education, body mass index (BMI), sleep medication use and the ApoE4 status), while dependent variables were neuroimaging signal values, each modality being tested separately.

2.5.3. Partial correlation analyses

Finally, partial correlations were performed on the whole sample of participants in order to assess potential associations between (i) the three measures of SDB severity, and (ii) SDB-related brain changes, with cognitive and behavioral variables. These analyses were controlled for age, sex, education, BMI, sleep medication use and ApoE4 status, and considered significant at a P<.05 threshold, after applying a Bonferroni correction for multiple comparisons. Thus, the statistical threshold for significance was set to P≤(.05/number of comparisons).

3. Results

3.1. Participants' characteristics

Participants' characteristics, including demographical and behavioral variables, neuropsychological scores, sleep parameters, as well as corresponding between-group differences, are provided in **Table 1**. SDB+ and SDB- participants did not differ for age, sex, education, depression and anxiety scores, current use of sleep medication, and the proportion of ApoE4 carriers. As expected, SDB+ participants presented significantly higher BMI (t=2.25; mean difference=1.96; 95% CI, 0.23 to 3.69; P=.03), AHI (t=8.64; mean difference=20.91; 95% CI, 16.12 to 25.70; P<.001), levels of sleep fragmentation (t=5.96; mean difference=0.90; 95% CI, 0.60 to 1.20; P<.001), and hypoxia (t=3.68; mean

difference=0.59; 95% CI, 0.27 to 0.91; P<.001). Interestingly, no between-group difference was observed for subjective sleep quality, daytime sleepiness symptoms, objectively-measured total sleep time, sleep efficiency, and sleep onset latency on the PSG night. Moreover, cognitive performance and self-reported cognitive difficulties were comparable between the two groups.

3.2. Brain changes associated with the presence of SDB

Results of between-group comparisons for MRI and PVE-corrected PET data are presented in **Figure 2**, and cluster peak statistics and coordinates are detailed in eTable 1 in the Supplement.

SDB+ participants presented greater amyloid burden in the left precuneus, posterior cingulate, calcarine, and cuneus regions (**Figure 2A;** T=4.51; $P_{FWE\text{-}corrected}$=.04; Cohen's d=0.83), compared to SDB- participants. They also showed greater GM volume in the precuneus and posterior cingulate cortex, bilaterally (**Figure 2B**; T=4.12; $P_{FWE\text{-}corrected}$=.04; Cohen's d=0.75), and greater perfusion in parieto-occipital regions, including the precuneus, posterior cingulate, calcarine, and lingual areas (**Figure 2C**; T=4.62; $P_{FWE\text{-}corrected}$=.001; Cohen's d=0.86). Finally, SDB+ participants presented greater glucose metabolism in the precuneus, posterior cingulate, and lingual areas, bilaterally (**Figure 2D**; T=4.63; $P_{FWE\text{-}corrected}$=.001; Cohen's d=1.04). Additionally, we further compared brain changes between participants with moderate SDB (i.e., 15≤AHI<30) *versus* severe SDB (AHI≥30), and found no significant differences at the p<.005 level, combined with a FWE cluster-level correction (data not shown). This suggests that brain changes associated with SDB are detectable from the moderate stage, and are not exacerbated in participants with severe SDB.

Interestingly, there was an overlap between brain changes observed in all four neuroimaging modalities over the posterior cingulate cortex, the precuneus and the cuneus **(Figure 3)**.

Perfusion, metabolism and GM volume signal values extracted from significant clusters showed strong inter-correlations, and amyloid deposition significantly correlated with GM volume and perfusion (eTable 2 in the Supplement).

Lastly, for the sake of completeness, region of interest (ROI)-based complementary analyses were performed. The signal was extracted from PVE-corrected and uncorrected FDG, early and late Florbetapir PET images, in ROIs from the AAL atlas[33] overlapping with the significant clusters obtained in the voxel-wise analyses. The results are summarized in the eTable 3 in the Supplement, and are overall consistent with the findings from the voxel-wise analyses. Only results obtained with PVE-uncorrected amyloid PET images were less significant, which likely reflect the between-group differences in GM volume highlighted in the main analyses.

3.3. Links between SDB-related brain changes and measures of SDB severity.

Forward stepwise regressions were then performed in order to determine which aspect of SDB severity is the most predictive of SDB-related brain changes **(Table 2)**. The best predictors of amyloid burden were the hypoxia composite score, explaining 8% of the variance (unstandardized β=.06; 95% CI, .02 to .10; P=.002), followed by the ApoE4 status, explaining 4% of the variance (unstandardized β=.07; 95% CI, .001 to .14; P=.05). No other variable entered the model. The AHI was the only predictive variable of GM volume, explaining 4% of the variance (unstandardized β=.01; P=.04). No variable significantly predicted brain perfusion or metabolism.

To ensure that these findings were not biased by a possible circularity issue, we replicated stepwise regression analyses with neuroimaging values that were independent from the previous between-group comparison. For this purpose, amyloid deposition was more globally measured through the global neocortical SUVr, and GM volume was extracted from the

composite ROI of posterior regions of the AAL atlas described above (eTable 4 in the Supplement). Briefly, results were similar for amyloid burden, with hypoxia severity being the best predictor of the global neocortical amyloid SUVr (unstandardized β=.06; 95% CI, .01 to .11; P=.01), followed by the APOE4 status (unstandardized β=.09; 95% CI, .01 to .17; P=.04). Moreover, the AHI was still the best SDB-related predictor of GM volume, although it was preceded by the BMI, sex and age.

3.4. Links with cognition, self-reported cognitive and sleep difficulties

Lastly, we aimed at exploring the cognitive and behavioral correlates of SDB severity and associated brain changes. No association survived the Bonferroni correction for multiple comparisons (eTable 5 in the Supplement), such that neither measures of SDB severity, nor SDB-related brain changes, were related to cognitive performance, self-reported cognitive and sleep difficulties or symptoms of sleepiness.

4. Discussion

The main goal of the present study was to provide a comprehensive overview of brain changes associated with untreated SDB in community-dwelling older participants with few symptoms. Our results show that SDB+ participants presented greater amyloid burden, GM volume, metabolism, and perfusion in parieto-occipital regions, including the precuneus and posterior cingulate cortex. Interestingly, greater amyloid burden was robustly associated with the severity of hypoxia. Neither SDB severity, nor SDB-related brain changes, were associated with cognitive performance, self-reported cognitive and sleep difficulties, and symptoms of sleepiness.

The association between SDB and greater amyloid deposition is in line with previous studies showing that SDB is associated with lower serum and CSF amyloid levels[18,20]. Furthermore, our results characterize the regional pattern of amyloid deposition in cognitively unimpaired individuals with SDB, extending the findings of Yun and colleagues[23] to a larger and older sample of individuals. The association between amyloid deposition and hypoxia severity is also consistent with animal studies, showing that hypoxia promotes the cleavage of the amyloid precursor protein by the β- and γ-secretases, leading to increased Aβ levels[34–36]. Moreover, it may partly explain why this specific aspect of SDB, rather than the AHI or sleep fragmentation, significantly predicts cognitive decline and conversion to Alzheimer's clinical syndrome in older adults[6,37].

Interestingly, SDB+ participants also presented greater GM volume, perfusion, and metabolism, in line with the findings of several other studies[12,15,17,38,39]. Nevertheless, other groups have also reported GM atrophy, hypoperfusion and hypometabolism in participants with SDB[9–11,14,16]. Discrepancies across studies may be due, at least in part, to methodological differences, as most studies have been performed on smaller samples of young and middle-aged participants with severe SDB (AHI>30). Alternatively, it is possible that studies including participants with less severe SDB (i.e., from the moderate stage, corresponding to an AHI>15) and few symptoms, as in the present study and in others[12,15], may be more able to capture earlier brain changes associated with the presence of SDB.

Greater GM volume, perfusion and metabolism observed in SDB+ participants could result from astrogliosis, microgliosis, and neuro-inflammatory processes[38,40–42]. Importantly, our results show for the first time, *in vivo*, that greater amyloid burden co-localize with greater GM volume, perfusion, and metabolism in cognitively unimpaired older participants with SDB. We believe that these overlapping patterns reinforce the likelihood of common

underlying mechanisms. Indeed, it has been demonstrated that higher neuronal activity is associated with increased Aβ production[43–46]. In addition, several studies have shown that neuro-inflammatory processes play a central role in AD progression, and are associated with higher levels of amyloid deposition[47]. Thus, SDB-related neuro-inflammatory processes and associated neuronal hyperactivity are likely to promote amyloid deposition in the same area. Furthermore, greater GM volume, perfusion and metabolism co-localizing with amyloid deposition may precede the development of neuronal injury, such as hypometabolism, and atrophy[48,49]. Alternatively, greater GM volume, perfusion and metabolism could also reflect higher brain reserve[50], helping to cope with amyloid pathology and maintain cognitive performance.

In our study, SDB-related brain changes were not associated with cognitive performance, self-reported cognitive and sleep difficulties, or symptoms of excessive daytime sleepiness. We believe that this finding indicates that greater amyloid deposition, GM volume, perfusion, and metabolism may represent early and asymptomatic brain changes associated with SDB. Studies exploring the associations between SDB and cognitive performance using cross-sectional designs have provided mixed results[7,51–53], but longitudinal studies showed that SDB is associated with conversion to Alzheimer's clinical syndrome, and with cognitive decline over time[6–8]. Therefore, older adults with SDB may exhibit silent brain changes, including increased amyloid deposition, which may propagate with time and explain why they are more at risk of developing Alzheimer's clinical syndrome.

The main strengths of the present study are the multimodal assessment of brain integrity, allowing to reveal the overlap of brain changes, and the detailed cognitive assessment, on a large sample of cognitively unimpaired older individuals. However, the cross-sectional design

of the analyses does not allow for the assessment of the causal relationships between SDB and brain changes, and longitudinal studies are needed to investigate whether these early SDB-related brain changes will progress to neurodegeneration and cognitive deficits.

Taken together, community-dwelling older individuals with untreated SDB presented greater amyloid deposition, GM volume, perfusion and metabolism mainly over the posterior cingulate, cuneus and precuneus areas, typically altered in AD. However, no association with cognitive performance, self-reported cognitive or sleep difficulties, or sleepiness symptoms was observed. Early neuro-inflammatory and neuronal hyperactivity processes promoting amyloid deposition could represent the underlying mechanisms increasing the susceptibility to AD at an asymptomatic stage of SDB. Our findings highlight the need to treat sleep disorders in the older population, even in the absence of cognitive or behavioral manifestations.

5. Acknowledgements

The authors are grateful to Alison Mary, Franck Doidy, Sébastien Polvent, Nicolas Oulhaj, Aurélia Cognet, Clarisse Gaubert, and the Cyceron MRI-PET staff for their help with recruitment and data acquisition or administrative support, as well as Caitlin Ware for editing the final draft. We acknowledge the members of the Medit-Ageing Research Group, Euclid team, the sponsor (Pôle de Recherche Clinique at Inserm), and all the participants of the study for their contribution.

The Age-Well RCT is part of the Medit-Ageing project funded through the European Union's Horizon 2020 research and innovation program (grant agreement N°667696), INSERM, Région Normandie, and Fondation d'entreprise MMA des Entrepreneurs du Futur. CA was funded by INSERM, Région Normandie, and the Fonds Européen de Développement

Régional (FEDER). Complementary funding sources were obtained from the Fondation LECMA-Vaincre Alzheimer (grant n°13732) and the Fondation Thérèse et René Planiol. Funding sources were not involved in the design and conduct of the study; collection, management, analysis and interpretation of the data; preparation, review, or approval of the manuscript; and decision to submit the manuscript for publication. Drs Chételat and Rauchs had full access to all the data in the study and take responsibility for the integrity of the data and the accuracy of the data analysis.

6. References

1. Berry RB, Brooks R, Gamaldo C, et al. AASM Scoring Manual Updates for 2017 (Version 2.4). *J Clin Sleep Med*. 2017;13(05):665-666. doi:10.5664/jcsm.6576
2. Malhotra A, White DP. Obstructive sleep apnoea. *Lancet*. 2002;360(9328):237-245. doi:10.1016/S0140-6736(02)09464-3
3. Ancoli-Israel S, Kripke D, Mason W, Messin S. Comparisons of Home Sleep Recordings and Polysomnograms in Older Adults with Sleep Disorders. *Sleep*. 1981;4(3):283-291. doi:10.1093/sleep/4.3.283
4. Senaratna C V., Perret JL, Lodge CJ, et al. Prevalence of obstructive sleep apnea in the general population: A systematic review. *Sleep Med Rev*. 2017;34:70-81. doi:10.1016/j.smrv.2016.07.002
5. Emamian F, Khazaie H, Tahmasian M, et al. The Association Between Obstructive Sleep Apnea and Alzheimer's Disease: A Meta-Analysis Perspective. *Front Aging Neurosci*. 2016;8. doi:10.3389/fnagi.2016.00078
6. Yaffe K, Laffan AM, Harrison SL, et al. Sleep-Disordered Breathing, Hypoxia, and Risk of Mild Cognitive Impairment and Dementia in Older Women. *JAMA*. 2011;306(6):613-619. doi:10.1001/jama.2011.1115

7. Leng Y, McEvoy CT, Allen IE, Yaffe K. Association of Sleep-Disordered Breathing With Cognitive Function and Risk of Cognitive Impairment: A Systematic Review and Meta-analysis. *JAMA Neurol*. 2017;74(10):1237-1245. doi:10.1001/jamaneurol.2017.2180

8. Osorio RS, Gumb T, Pirraglia E, et al. Sleep-disordered breathing advances cognitive decline in the elderly. *Neurology*. 2015;84(19):1964-1971. doi:10.1212/WNL.0000000000001566

9. Huang X, Tang S, Lyu X, Yang C, Chen X. Structural and functional brain alterations in obstructive sleep apnea: a multimodal meta-analysis. *Sleep Med*. 2019;54:195-204. doi:10.1016/j.sleep.2018.09.025

10. Shi Y, Chen L, Chen T, et al. A Meta-analysis of Voxel-based Brain Morphometry Studies in Obstructive Sleep Apnea. *Sci Rep*. 2017;7(1):10095. doi:10.1038/s41598-017-09319-6

11. Tahmasian M, Rosenzweig I, Eickhoff SB, et al. Structural and functional neural adaptations in obstructive sleep apnea: An activation likelihood estimation meta-analysis. *Neurosci Biobehav Rev*. 2016;65:142-156. doi:10.1016/j.neubiorev.2016.03.026

12. Baril A-A, Gagnon K, Brayet P, et al. Gray Matter Hypertrophy and Thickening with Obstructive Sleep Apnea in Middle-aged and Older Adults. *Am J Respir Crit Care Med*. 2017;195(11):1509-1518. doi:10.1164/rccm.201606-1271OC

13. Rosenzweig I, Kempton MJ, Crum WR, et al. Hippocampal Hypertrophy and Sleep Apnea: A Role for the Ischemic Preconditioning? Annunziato L, ed. *PLoS One*. 2013;8(12):e83173. doi:10.1371/journal.pone.0083173

14. Innes CRH, Kelly PT, Hlavac M, Melzer TR, Jones RD. Decreased Regional Cerebral Perfusion in Moderate-Severe Obstructive Sleep Apnoea during Wakefulness. *Sleep*.

2015;38(5):699-706. doi:10.5665/sleep.4658

15. Baril A-A, Gagnon K, Arbour C, et al. Regional Cerebral Blood Flow during Wakeful Rest in Older Subjects with Mild to Severe Obstructive Sleep Apnea. *Sleep*. 2015;38(9):1439-1449. doi:10.5665/sleep.4986

16. Kim JS, Seo JH, Kang M-R, et al. Effect of continuous positive airway pressure on regional cerebral blood flow in patients with severe obstructive sleep apnea syndrome. *Sleep Med*. 2017;32:122-128. doi:10.1016/j.sleep.2016.03.010

17. Nie S, Peng D-C, Gong H-H, Li H-J, Chen L-T, Ye C-L. Resting cerebral blood flow alteration in severe obstructive sleep apnoea: an arterial spin labelling perfusion fMRI study. *Sleep Breath*. 2017;21(2):487-495. doi:10.1007/s11325-017-1474-9

18. Bu X-L, Liu Y-H, Wang Q-H, et al. Serum amyloid-beta levels are increased in patients with obstructive sleep apnea syndrome. *Sci Rep*. 2015;5(1):13917. doi:10.1038/srep13917

19. Bubu OM, Pirraglia E, Andrade AG, et al. Obstructive sleep apnea and longitudinal Alzheimer's disease biomarker changes. *Sleep*. 2019;42(6). doi:10.1093/sleep/zsz048

20. Liguori C, Mercuri NB, Izzi F, et al. Obstructive Sleep Apnea is Associated With Early but Possibly Modifiable Alzheimer's Disease Biomarkers Changes. *Sleep*. 2017;40(5). doi:10.1093/sleep/zsx011

21. Sharma RA, Varga AW, Bubu OM, et al. Obstructive Sleep Apnea Severity Affects Amyloid Burden in Cognitively Normal Elderly. A Longitudinal Study. *Am J Respir Crit Care Med*. 2018;197(7):933-943. doi:10.1164/rccm.201704-0704OC

22. Elias A, Cummins T, Tyrrell R, et al. Risk of Alzheimer's Disease in Obstructive Sleep Apnea Syndrome: Amyloid-β and Tau Imaging. *J Alzheimer's Dis*. 2018;66(2):733-741. doi:10.3233/JAD-180640

23. Yun C-H, Lee H-Y, Lee SK, et al. Amyloid Burden in Obstructive Sleep Apnea. *J*

Alzheimer's Dis. 2017;59(1):21-29. doi:10.3233/JAD-161047

24. Spira AP, Yager C, Brandt J, et al. Objectively Measured Sleep and β-amyloid Burden in Older Adults: A Pilot Study. *SAGE open Med*. 2014;2. doi:10.1177/2050312114546520

25. Poisnel G, Arenaza-Urquijo E, Collette F, et al. The Age-Well randomized controlled trial of the Medit-Ageing European project: Effect of meditation or foreign language training on brain and mental health in older adults. *Alzheimer's Dement Transl Res Clin Interv*. 2018;4:714-723. doi:10.1016/j.trci.2018.10.011

26. McNair DM, Kahn RJ, Crook T, Ferris S, Bartus R. *Assessment in Geriatric Psychopharmacology*. Mark Powle. New Canaan, Connecticut; 1983.

27. Buysse DJ, Reynolds CF, Monk TH, Berman SR, Kupfer DJ. The Pittsburgh Sleep Quality Index: a new instrument for psychiatric practice and research. *Psychiatry Res*. 1989;28(2):193-213. doi:10.1016/0165-1781(89)90047-4

28. Johns MW. A new method for measuring daytime sleepiness: the Epworth sleepiness scale. *Sleep*. 1991;14(6):540-545. doi:10.1093/sleep/14.6.540

29. Müller-Gärtner HW, Links JM, Prince JL, et al. Measurement of radiotracer concentration in brain gray matter using positron emission tomography: MRI-based correction for partial volume effects. *J Cereb Blood Flow Metab*. 1992;12(4):571-583. doi:10.1038/jcbfm.1992.81

30. Sateia MJ. International classification of sleep disorders-third edition highlights and modifications. *Chest*. 2014;146(5):1387-1394. doi:10.1378/chest.14-0970

31. Ju Y-ES, Finn MB, Sutphen CL, et al. Obstructive sleep apnea decreases central nervous system-derived proteins in the cerebrospinal fluid. *Ann Neurol*. 2016;80(1):154-159. doi:10.1002/ana.24672

32. Osorio RS, Ayappa I, Mantua J, et al. The interaction between sleep-disordered

breathing and apolipoprotein E genotype on cerebrospinal fluid biomarkers for Alzheimer's disease in cognitively normal elderly individuals. *Neurobiol Aging*. 2014;35(6):1318-1324. doi:10.1016/j.neurobiolaging.2013.12.030

33. Tzourio-Mazoyer N, Landeau B, Papathanassiou D, et al. Automated anatomical labeling of activations in SPM using a macroscopic anatomical parcellation of the MNI MRI single-subject brain. *Neuroimage*. 2002;15(1):273-289. doi:10.1006/nimg.2001.0978

34. Sun X, He G, Qing H, et al. Hypoxia facilitates Alzheimer's disease pathogenesis by up-regulating BACE1 gene expression. *Proc Natl Acad Sci U S A*. 2006;103(49):18727-18732. doi:10.1073/pnas.0606298103

35. Li L, Zhang X, Yang D, Luo G, Chen S, Le W. Hypoxia increases Abeta generation by altering beta- and gamma-cleavage of APP. *Neurobiol Aging*. 2009;30(7):1091-1098. doi:10.1016/j.neurobiolaging.2007.10.011

36. Shiota S, Takekawa H, Matsumoto S-E, et al. Chronic intermittent hypoxia/reoxygenation facilitate amyloid-β generation in mice. *J Alzheimers Dis*. 2013;37(2):325-333. doi:10.3233/JAD-130419

37. Blackwell T, Yaffe K, Laffan A, et al. Associations between sleep-disordered breathing, nocturnal hypoxemia, and subsequent cognitive decline in older community-dwelling men: the Osteoporotic Fractures in Men Sleep Study. *J Am Geriatr Soc*. 2015;63(3):453-461. doi:10.1111/jgs.13321

38. Rosenzweig I, Williams SCR, Morrell MJ. The impact of sleep and hypoxia on the brain: potential mechanisms for the effects of obstructive sleep apnea. *Curr Opin Pulm Med*. 2014;20(6):565-571. doi:10.1097/MCP.0000000000000099

39. Cross NE, Memarian N, Duffy SL, et al. Structural brain correlates of obstructive sleep apnoea in older adults at risk for dementia. *Eur Respir J*. 2018;52(1):1800740.

doi:10.1183/13993003.00740-2018

40. Aviles-Reyes RX, Angelo MF, Villarreal A, Rios H, Lazarowski A, Ramos AJ. Intermittent hypoxia during sleep induces reactive gliosis and limited neuronal death in rats: implications for sleep apnea. *J Neurochem*. 2010;112(4):854-869. doi:10.1111/j.1471-4159.2009.06535.x

41. Li K, Zhang J, Qin Y, Wei Y-X. Association between Serum Homocysteine Level and Obstructive Sleep Apnea: A Meta-Analysis. *Biomed Res Int*. 2017;2017:7234528. doi:10.1155/2017/7234528

42. Daulatzai MA. Death by a Thousand Cuts in Alzheimer's Disease: Hypoxia—The Prodrome. *Neurotox Res*. 2013;24(2):216-243. doi:10.1007/s12640-013-9379-2

43. Bero AW, Yan P, Roh JH, et al. Neuronal activity regulates the regional vulnerability to amyloid-β deposition. *Nat Neurosci*. 2011;14(6):750-756. doi:10.1038/nn.2801

44. Raichle ME, MacLeod AM, Snyder AZ, Powers WJ, Gusnard DA, Shulman GL. A default mode of brain function. *Proc Natl Acad Sci*. 2001;98(2):676-682. doi:10.1073/pnas.98.2.676

45. Buckner RL, Sepulcre J, Talukdar T, et al. Cortical Hubs Revealed by Intrinsic Functional Connectivity: Mapping, Assessment of Stability, and Relation to Alzheimer's Disease. *J Neurosci*. 2009;29(6):1860-1873. doi:10.1523/JNEUROSCI.5062-08.2009

46. Cirrito JR, Yamada KA, Finn MB, et al. Synaptic Activity Regulates Interstitial Fluid Amyloid-β Levels In Vivo. *Neuron*. 2005;48(6):913-922. doi:10.1016/j.neuron.2005.10.028

47. Kinney JW, Bemiller SM, Murtishaw AS, Leisgang AM, Salazar AM, Lamb BT. Inflammation as a central mechanism in Alzheimer's disease. *Alzheimer's Dement Transl Res Clin Interv*. 2018;4:575-590. doi:10.1016/j.trci.2018.06.014

48. Fortea J, Vilaplana E, Alcolea D, et al. Cerebrospinal fluid β-amyloid and phospho-tau biomarker interactions affecting brain structure in preclinical Alzheimer disease. *Ann Neurol*. 2014;76(2):223-230. doi:10.1002/ana.24186

49. Pegueroles J, Vilaplana E, Montal V, et al. Longitudinal brain structural changes in preclinical Alzheimer's disease. *Alzheimer's Dement*. 2017;13(5):499-509. doi:10.1016/j.jalz.2016.08.010

50. Stern Y, Arenaza-Urquijo EM, Bartrés-Faz D, et al. Whitepaper: Defining and investigating cognitive reserve, brain reserve, and brain maintenance. *Alzheimer's Dement*. 2018. doi:10.1016/j.jalz.2018.07.219

51. Olaithe M, Bucks RS, Hillman DR, Eastwood PR. Cognitive deficits in obstructive sleep apnea: Insights from a meta-review and comparison with deficits observed in COPD, insomnia, and sleep deprivation. *Sleep Med Rev*. 2018;38:39-49. doi:10.1016/j.smrv.2017.03.005

52. Boland LL, Shahar E, Iber C, et al. Measures of cognitive function in persons with varying degrees of sleep-disordered breathing: the Sleep Heart Health Study. *J Sleep Res*. 2002;11(3):265-272. http://www.ncbi.nlm.nih.gov/pubmed/12220323.

53. Sforza E, Roche F, Thomas-Anterion C, et al. Cognitive Function and Sleep Related Breathing Disorders in a Healthy Elderly Population: the Synapse Study. *Sleep*. 2010;33(4):515-521. doi:10.1093/sleep/33.4.515

Figures.

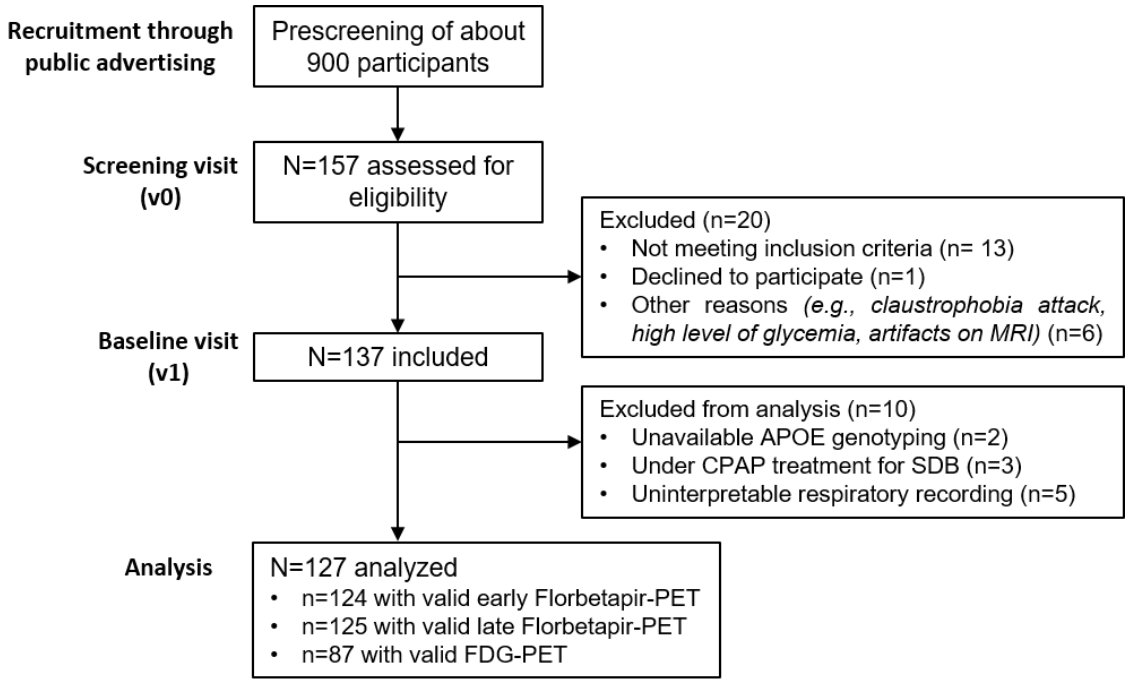


Figure 1: Flow diagram of the inclusion process.

Abbreviations: APOE, Apolipoprotein E; FDG, ^{18}F-fluorodeoxyglucose; MRI, Magnetic Resonance Imaging; PET, Positons Emission Tomography

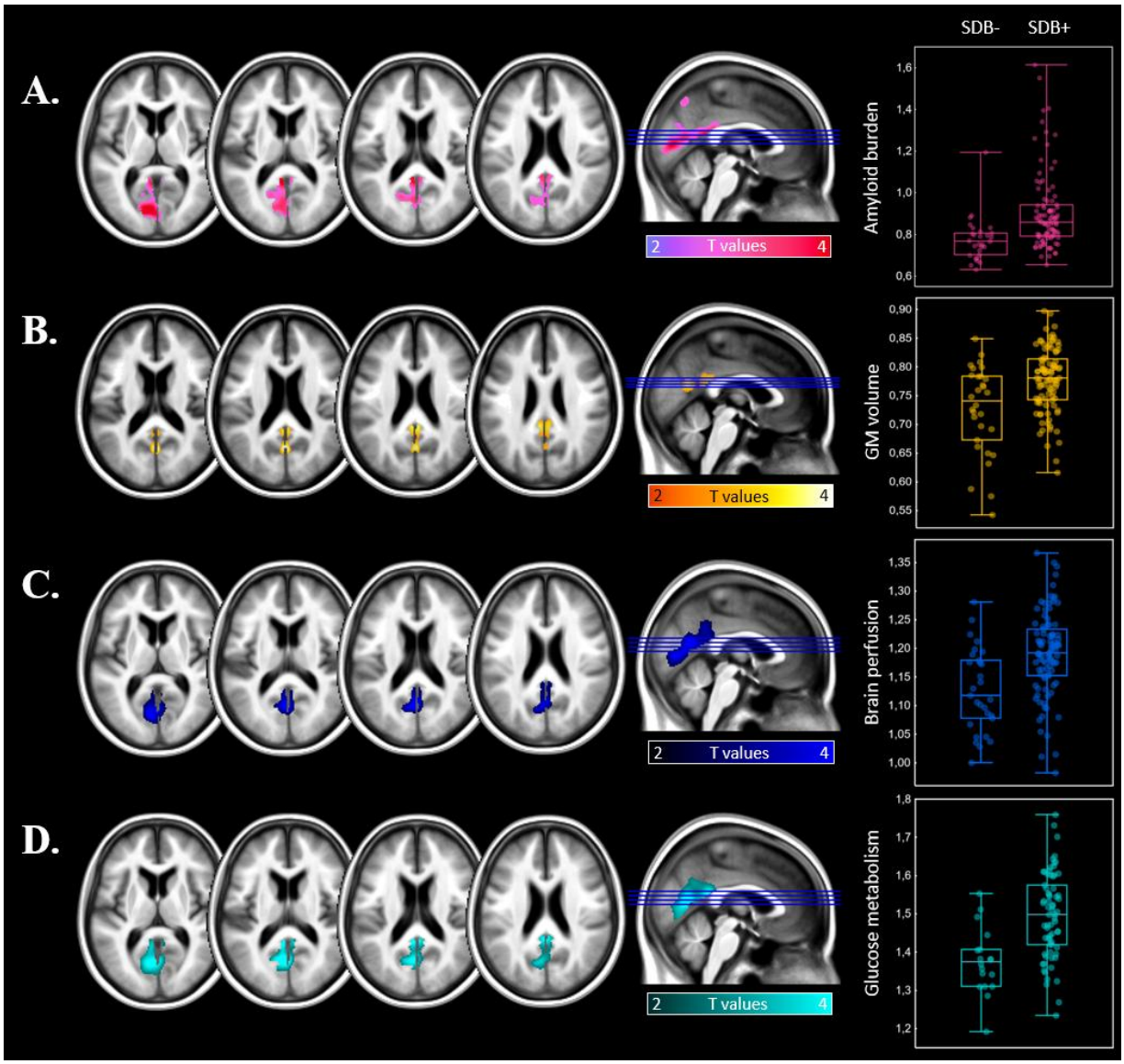


Figure 2: Neuroimaging pattern of the significant differences between SDB+ and SDB- participants in amyloid deposition, GM volume, perfusion, and glucose metabolism.

Abbreviations: APOE, Apolipoprotein E; GM, gray matter; SDB, sleep-disordered breathing.

Results of the voxel-wise ANCOVAs exhibiting between-group differences in **(A)** amyloid deposition, **(B)** GM volume, **(C)** perfusion, and **(D)** glucose metabolism, using MRI and PVE-corrected PET data. Analyses were adjusted for age, sex, education, body mass index, sleep medication use, and the ApoE4 status. Results were obtained at a P<.005 (uncorrected) threshold, and only clusters surviving a FWE cluster-level correction are reported.

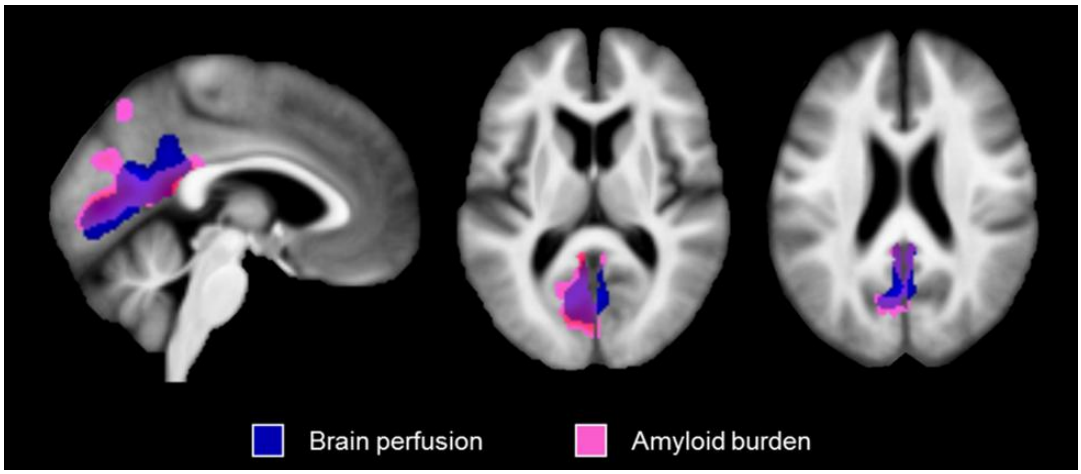


Figure 3: Overlap of SDB-related brain changes in SDB+ compared to SDB- participants.

Abbreviations: FWE, family-wise error; GM, gray matter.

Representation of the overlap between SDB-related patterns of greater perfusion (blue) and amyloid deposition (pink), obtained at a P<.005 (uncorrected) threshold combined with a FWE cluster-level correction.

Tables.

Table 1: Participant characteristics and between-group differences.

	SDB- (n=31)	SDB+ (n=96)	Between-group differences [a]
Demographics			
Age: years	69.19 (3.53)	69.00 (3.98)	p=.81
Sex: number (%) of women	24 (77.4%)	56 (58.3%)	p=.06
Education: years	13.45 (2.94)	12.90 (3.12)	p=.38
GDS: total score	1.55 (1.89)	1.21 (1.70)	p=.35
STAI-B: total score	36.13 (7.35)	34.05 (6.88)	p=.15
Body mass index: kg/m²	**24.77 (5.07)**	**26.73 (3.92)**	**p=.03**
Current sleep medication use: number (%) of users [b]	2 (6.45%)	10 (10.42%)	p=.51
Florbetapir SUVr: mean value (SD; % positive) [c]	0.91 (0.13; 10%)	0.99 (0.23; 25%)	p=.07
ApoE4: number (%) of carriers	9 (29.03%)	26 (27.08%)	p=.83
Sleep			
PSQI: total score	4.39 (2.67)	5.17 (3.16)	p=.22
ESS: total score	4.77 (3.04)	5.22 (3.45)	p=.52
TST: min	358.63 (59.13)	362.81 (67.62)	p=.76
Sleep efficiency: %	76.39 (10.24)	77.36 (9.89)	p=.64
Sleep onset latency: min	18.73 (12.41)	21.12 (12.49)	p=.35
Apnea-hypopnea index: number per hour	**9.63 (3.91)**	**30.54 (13.26)**	**p<.001**
Fragmentation: composite score	**-0.68 (0.41)**	**0.22 (0.81)**	**p<.001**
Respiratory arousals index: number per hour	**7.15 (3.34)**	**25.28 (11.30)**	**p<.001**
Shifts to NREM-1: number per hour	**5.81 (2.08)**	**8.39 (3.53)**	**p=.001**
Awakenings: number per hour	**3.29 (1.12)**	**4.11 (1.72)**	**p=.02**
Hypoxia: composite score [d]	**-0.44 (0.39)**	**0.15 (0.85)**	**p<.001**
Oxygen desaturation ≥3% index: number per hour	**5.50 (3.96)**	**16.50 (11.21)**	**p<.001**
TST with oxygen saturation ≤90%: %	0.50 (1.08)	2.88 (9.69)	p=.18
Minimal oxygen saturation: %	**88.27 (3.82)**	**85.89 (5.05)**	**p=.02**
Cognition			
MMSE: total score	28.81 (1.08)	29.06 (1.04)	p=.24
MDRS: total score	140.61 (2.89)	141.17 (2.64)	p=.32
Processing speed: composite score	0.05 (0.85)	-0.02 (0.70)	p=.66
Attention: composite score	-0.04 (0.66)	0.04 (0.63)	p=.58
Executive functioning: composite score	0.12 (0.70)	-0.04 (0.67)	p=.26
Working memory: composite score	0.04 (1.03)	-0.03 (0.85)	p=.72
Episodic memory: composite score	0.16 (0.81)	-0.05 (0.69)	p=.17
Cognitive Difficulties Scale: total score	33.84 (14.27)	34.18 (15.59)	p=.91

Abbreviations: ESS, Epworth Sleepiness Scale; GDS, Geriatric Depression Scale; MDRS: Mattis Dementia Rating Scale; MMSE, Mini Mental State Examination; NREM-1: non-rapid eye movement sleep stage 1; ns, non-significant; PSQI, Pittsburgh Sleep Quality Index; SD,

standard deviation; SDB, sleep-disordered breathing; STAI-B, State-Trait Inventory form B; SUVr, Standard Uptake Value ratio; TST, Total Sleep Time.

Results are expressed as means (SD), unless otherwise specified.

[a] Between-group differences were assessed using Student t-tests for continuous variables, and chi-square statistics for categorical variables. Statistical significance was set to P<.05.

[b] Use of sleep medication on a regular basis (>1/week), excluding phytotherapy and homeopathy.

[c] n=30 controls with valid Florbetapir-PET scan. The threshold for amyloid positivity was defined as >.99, and corresponded to the 99.9^{th} percentile of the neocortical SUVr distribution among 45 healthy young individuals, aged <40 years.

[d] n=30 SDB- and 88 SDB+ participants with valid data related to oxygen saturation.

Table 2: Forward stepwise regressions predicting SDB-related brain changes.

Dependent variable	Model	Predictor	Unstandardized coefficient	Standardized coefficient	95% CI	R^2	P-value
Amyloid burden	1	(intercept)	0.88		[0.85 – 0.91]		<.001
		Hypoxia composite	0.06	0.28	[0.02 – 0.10]	0.08	.002
	2	(intercept)	0.86		[0.82 – 0.90]		<.001
		Hypoxia composite	0.06	0.26	[0.02 – 0.10]		.004
		APOE4 status	0.07	0.18	[0.001 – 0.14]	0.11	.05
	Full model					0.16	.02
GM volume	1	(intercept)	0.77		[0.76 – 0.78]		<.001
		AHI	0.01	0.19	[5.718×10^{-4} – 0.02]	0.04	.04
	Full model					0.11	.20

Abbreviations: AHI, apnea-hypopnea index; APOE; apolipoprotein E; GM, gray matter.

Supplementary Online Content

André C, Rehel S, Kuhn E, et al; for the Medit-Ageing Research Group. Association of sleep-disordered breathing with Alzheimer disease biomarkers in community-dwelling older adults. *JAMA Neurol*. Published online March 23, 2020. doi:10.1001/jamaneurol.2020.0311

eAppendix. Methods

eTable 1. Detailed statistics of significant neuroimaging clusters.

eTable 2. Results of inter-modality correlations.

eTable 3. Results of between-group comparisons using a ROI approach for PET data.

eTable 4. Results of complementary forward stepwise regression analyses.

eTable 5. Results of partial correlation analyses between SDB parameters and SDB-related brain changes with cognitive and behavioural scores.

eReferences.

This supplementary material has been provided by the authors to give readers additional information about their work.

eAppendix. Methods

Neuropsychological scores

To obtain robust proxies of cognitive abilities and minimize the issue of multiple statistical testing, composite scores were used for each cognitive domain, instead of multiple (sub)tests. For that purpose, performance on various cognitive tests were z-transformed and averaged as follows. Please note that before averaging, Z-scores derived from reaction times and percentages/number of error were reversed so that increasing values always indicated better performance.

- Processing speed
  - Time to perform the Trail Making test (TMT) part A.
  - Time to complete the word card from the Stroop test (reading condition).
  - Time to complete the color card from the Stroop test (naming condition).

- Attention
  - Attention sub-score from the Mattis Dementia Rating Scale.
  - Number of correct items at the D2R test.
  - Percentage of errors at the D2R test.

- Executive functions
  - TMT test (time difference between TMT part B and part A, divided by the time to perform part A).
  - Stroop test (time difference between the interference and naming conditions).
  - Verbal fluency (number of words beginning with ‘‘p’’ in 2 min).

- Working memory
  - Digit span forward from the WAIS IV.
  - Digit span backward from the WAIS IV.
  - Digit span forward + backward total raw note from the WAIS IV.

- Episodic memory
  - Memory subscore from the Mattis Dementia Rating Scale.
  - Sum of the five free recalls from the learning trials of the California Verbal Learning Test (CVLT).
  - Short-term free recall from the CVLT.
  - Long-term free recall from the CVLT.
  - Long-term free recall from the Logical Memory Story test from the WMS IV.

Abbreviations: CVLT, California Verbal Learning Test; TMT, Trail Making Test; WAIS, Wechsler Adult Intelligence Scale; WMS, Weschler Memory Scale.

Neuroimaging procedure

All participants were scanned at the Cyceron Center (Caen, France) on the same MRI (Philips Achieva 3.0T scanner) and PET (Discovery RX VCT 64 PET-CT scanner, General Electric Healthcare) cameras. During the MRI session, subjects were equipped with earplugs and their head was stabilized with foam pads in order to minimize head motion.

1. *Structural MRI*

A high-resolution T1-weighted anatomical image was acquired using a 3D fast-field echo sequence (3D-T1-FFE sagittal, repetition time =7.1 ms, echo time = 3.3 ms, flip angle = 6°, 180 slices with no gap, slice thickness = 1mm, field of view = 256x256 mm^2, in-plane resolution= 1x1x1 mm^3). T1-weighted images were segmented using FLAIR images (3D-IR sagittal, TR/TE/TI = 4800/272/1650 ms ; flip angle = 40°; 180 slices with no gap; slice thickness = 1 mm; field of view = 250x250 mm^2; in-plane resolution = 0.98x0.98 mm^2), spatially normalized to the Montreal Neurological Institute (MNI) template, modulated using the SPM12 segmentation procedure (http://www.fil.ion.ucl.ac.uk) and smoothed with an 8 mm full-width at half-maximum (FWHM) Gaussian filter. Images were then masked to exclude non-grey matter voxels from the analyses.

2. *PET imaging*

Florbetapir- and FDG-PET scans were acquired in two separate sessions with a resolution of 3.76 × 3.76 × 4.9 mm^3 (field of view = 157 mm). Forty-seven planes were obtained with a voxel size of 1.95 × 1.95 × 3.27 mm^3. A transmission scan was performed for attenuation correction before the PET acquisition.
For the Florbetapir-PET scan, each participant underwent a 10 min PET scan beginning at the intravenous injection of ~4MBq/Kg of Florbetapir, and a 10 min PET scan beginning 50 min after the intravenous injection. Early Florbetapir-PET, reflecting brain perfusion, was reconstructed from 1 to 6 min. Late-Florbetapir acquisition reflected brain amyloid burden.
For the FDG-PET scan, participants (n=87) were fasted for at least 6 hours before scanning. After a 30-min resting period in a quiet and dark environment, 180 MBq of ^{18}F-fluorodeoxyglucose were intravenously injected as a bolus. A 10-min PET acquisition scan began 50 min after injection.
PET images were coregistered on their corresponding anatomical MRI, voxel-wise corrected for partial volume effects using the three-compartmental voxel-wise Müller-Gärtner method[1], and were then normalized to the MNI template using deformation parameters derived from the anatomical MRI. Resulting images were scaled using cerebellar grey matter as a reference. A smoothing kernel of 10 mm Gaussian filter was applied and images were masked to exclude non-grey matter voxels from the analyses. PVE-corrected normalized and scaled Florbetapir-PET images were also used to extract the individual global cortical amyloid standard uptake value ratio (SUVr) using a predetermined neocortical mask including the entire grey matter, except the cerebellum, occipital and sensory motor cortices, hippocampi, amygdala and basal nuclei[2]. The threshold for amyloid positivity was defined as >0.99, and corresponded to the 99.9th percentile of the neocortical SUVr distribution among 45 healthy young individuals, aged <40 years.

Polysomnography recording

Twenty EEG electrodes were placed over the scalp (Fp1, Fp2, F3, F4, F7, F8, Fz, C3, C4, Cz, T3, T4, P3, P4, Pz, O1, O2, vertex ground, and a bi-mastoid reference) according to the international 10-20 system, with impedances kept below 5 kΩ. Participants also underwent an electrooculogram, electrocardiogram, and chin electromyogram. Respiratory movements, airflow, and oxygen saturation were recorded respectively with thoracic and abdominal belts, nasal and oral thermistors, and a finger pulse oximeter. The EEG signal was digitalized at a sampling rate of 256 Hz. High-pass and low-pass filters were applied, respectively at 0.3Hz and 35Hz.

eTable 1. Detailed statistics of significant neuroimaging clusters.

	Cluster extent		MNI coordinates					
Brain areas	**voxels**	**mm^3**	**x**	**y**	**z**	**T-value**	**$p_{FWE\text{-}corrected}$**	**Effect size (Cohen's d)**
MRI								
B precuneus, posterior cingulate	829	2 798	0	-63	20	4.12	.04	.75
Early Florbetapir-PET								
L calcarine, L lingual, B precuneus, B posterior and middle cingulate	3 946	13 318	-6	-76	6	4.62	.001	.86
FDG-PET								
B calcarine, B lingual, B precuneus, B posterior cingulate	4 295	14 496	-3	-68	12	4.63	.001	1.04
Late Florbetapir-PET								
L calcarine, L precuneus, L posterior cingulate, L cuneus	4 699	15 859	-10	-78	6	4.51	.04	.83

Abbreviations: B, bilateral; FDG, ^{18}F-fluorodeoxyglucose, L, left; MNI, Montreal Neurological Institute; MRI: magnetic resonance imaging.
Results were obtained at a $p<0.005$ (uncorrected) threshold and only clusters surviving a FWE cluster-level correction are reported.

eTable 2. Results of inter-modality correlations.

Neuroimaging modality		Brain perfusion	Amyloid	Glucose metabolism	GM volume
Brain perfusion	Pearson's r	—			
	p-value	—			
	Upper 95% CI	—			
	Lower 95% CI	—			
Amyloid	Pearson's r	0.34	—		
	p-value	<.001	—		
	Upper 95% CI	0.49	—		
	Lower 95% CI	0.18	—		
Glucose metabolism	Pearson's r	0.70	0.15	—	
	p-value	<.001	.17	—	
	Upper 95% CI	0.80	0.35	—	
	Lower 95% CI	0.58	-0.06	—	
GM volume	Pearson's r	0.59	0.21	0.4	—
	p-value	<.001	.02	<.001	—
	Upper 95% CI	0.69	0.37	0.56	—
	Lower 95% CI	0.46	0.03	0.21	—

Neuroimaging signal values were extracted from significant clusters obtained in voxel-wise between-group comparisons. Please note that results remained unchanged when controlling for age, sex, education, body mass index, sleep medication use and APOE4 status (data not shown).

eTable 3. Results of between-group comparisons using a ROI approach for PET data.

Imaging modality	Region of Interest	F	p	Partial eta-squared
Late Florbetapir-PET (PVE-corrected)	**Composite**	**4.77**	**.03**	**0.04**
	PCC L	**4.88**	**.03**	**0.04**
	PCC R	**4.62**	**.03**	**0.04**
	Cuneus L	**7.07**	**.01**	**0.06**
	Cuneus R	**5.35**	**.02**	**0.04**
	Precuneus L	**4.23**	**.04**	**0.04**
	Precuneus R	**4.17**	**.04**	**0.03**
	Lingual L	**5.38**	**.02**	**0.04**
	Lingual R	0.66	.42	0.01
	Calcarine L	**8.81**	**.004**	**0.07**
	Calcarine R	3.45	.07	0.03
Late Florbetapir-PET (uncorrected for PVE)	Composite	3.85	.05	0.03
	PCC L	1.94	.17	0.02
	PCC R	1.59	.21	0.01
	Cuneus L	3.58	.06	0.03
	Cuneus R	**4.21**	**.04**	**0.04**
	Precuneus L	**4.03**	**.05**	**0.03**
	Precuneus R	3.85	.05	0.03
	Lingual L	**4.26**	**.04**	**0.04**
	Lingual R	2.61	.11	0.02
	Calcarine L	3.68	.06	0.03
	Calcarine R	3.59	.06	0.03
Early Florbetapir-PET (PVE-corrected)	**Composite**	**9.12**	**.003**	**0.07**
	PCC L	**8.90**	**.004**	**0.07**
	PCC R	**10.55**	**.002**	**0.08**
	Cuneus L	**4.88**	**.03**	**0.04**
	Cuneus R	3.00	.09	0.03
	Precuneus L	**6.34**	**.01**	**0.05**
	Precuneus R	**7.98**	**.01**	**0.06**
	Lingual L	**8.00**	**.01**	**0.06**
	Lingual R	**5.35**	**.02**	**0.04**
	Calcarine L	**12.50**	**.001**	**0.10**
	Calcarine R	**4.05**	**.05**	**0.03**
Early Florbetapir-PET (uncorrected for PVE)	**Composite**	**6.74**	**.01**	**0.06**
	PCC L	**7.41**	**.01**	**0.06**
	PCC R	**9.12**	**.003**	**0.07**
	Cuneus L	3.52	.06	0.03
	Cuneus R	2.90	.09	0.02
	Precuneus L	**5.23**	**.02**	**0.04**
	Precuneus R	**6.17**	**.01**	**0.05**
	Lingual L	**7.27**	**.01**	**0.06**
	Lingual R	**5.27**	**.02**	**0.04**
	Calcarine L	**8.58**	**.004**	**0.07**
	Calcarine R	**4.17**	**.04**	**0.04**
FDG-PET (PVE-corrected)	**Composite**	**6.98**	**.01**	**0.08**
	PCC L	**9.39**	**.003**	**0.11**
	PCC R	**10.31**	**.002**	**0.12**
	Cuneus L	**5.99**	**.02**	**0.07**
	Cuneus R	**5.28**	**.02**	**0.06**
	Precuneus L	**4.60**	**.04**	**0.06**
	Precuneus R	**5.70**	**.02**	**0.07**
	Lingual L	**4.90**	**.03**	**0.06**

	Lingual R	3.22	.08	0.04
	Calcarine L	**9.05**	**.004**	**0.10**
	Calcarine R	**4.13**	**.05**	**0.05**
FDG-PET (uncorrected for PVE)	**Composite**	**5.04**	**.03**	**0.06**
	PCC L	**7.78**	**.007**	**0.09**
	PCC R	**8.48**	**.005**	**0.10**
	Cuneus L	**4.69**	**.03**	**0.06**
	Cuneus R	**4.62**	**.04**	**0.06**
	Precuneus L	**4.01**	**.05**	**0.05**
	Precuneus R	**5.03**	**.03**	**0.06**
	Lingual L	3.56	.06	0.04
	Lingual R	2.68	.10	0.03
	Calcarine L	**5.62**	**.02**	**0.07**
	Calcarine R	3.66	.06	0.04

Abbreviations: AAL, Automated Anatomical Labelling; FDG, ^{18}F-fluorodeoxyglucose, L, left; PCC, posterior cingulate cortex; PVE, partial volume effect; R, right; ROI, region of interest.
Results of between-group comparisons (SDB+>SDB-) for amyloid burden (late Florbetapir-PET, n=125), brain perfusion (early Florbetapir-PET, n=124) and glucose metabolism (FDG-PET, n=87) data, extracted from PVE-corrected and uncorrected PET images in standardized ROIs of the AAL Atlas overlapping with the significant clusters obtained in the voxel-wise analyses. The "composite" ROI is a meta-ROI comprising all the individual AAL ROIs listed below (i.e., left and right PCC, cuneus, precuneus, lingual and calcarine regions). The statistical threshold for significance was set to $p<0.05$, and significant results are indicated in bold.

eTable 4. Results of complementary forward stepwise regression analyses.

Imaging modality	Model	Predictor	Unstandardized coefficient	Standardized coefficient	R^2	p	Lower 95% CI	Upper 95% CI
Neocortical amyloid SUVr	1	(Intercept)	0.97			<.001	0.94	1.01
		Hypoxia composite	0.06	0.23	0.05	.01	0.01	0.11
	2	(Intercept)	0.95			<.001	0.91	0.99
		Hypoxia composite	0.06	0.22		.02	0.01	0.10
		ApoE4 status	0.09	0.19	0.09	.04	0.01	0.17
	Full model				*0.13*	*.07*		
GM volume extracted from the composite AAL ROI	1	(Intercept)	0.72			< .001	0.68	0.76
		BMI	-0.003	-0.32	0.10	< .001	-0.004	-0.001
	2	(Intercept)	0.72			< .001	0.69	0.76
		BMI	-0.002	-0.31		< .001	-0.004	-0.001
		Sex	-0.02	-0.24	0.15	.01	-0.03	-0.005
	3	(Intercept)	0.83			< .001	0.72	0.94
		BMI	-0.003	-0.32		< .001	-0.004	-0.001
		Sex	-0.02	-0.23		.01	-0.03	-0.005
		Age	-0.002	-0.17	0.19	.05	-0.003	-6.404e -6
	4	(Intercept)	0.85			< .001	0.73	0.96
		BMI	-0.003	-0.34		< .001	-0.004	-0.001
		Sex	-0.02	-0.26		.002	-0.03	-0.007
		Age	-0.002	-0.19		.03	-0.003	-1.975e -4
		AHI	0.007	0.19	0.22	.03	6.235e -4	0.01
	Full model				*0.25*	*<.001*		

Abbreviations: AAL, Automated Anatomical Labelling; ROI, Region of Interest; SUVr, Standard Uptake Value ratio.

eTable 5. Results of partial correlation analyses between SDB parameters and SDB-related brain changes with cognitive and behavioural scores.

Cognitive and behavioral variables	SDB parameters			SDB-related brain changes			
	AHI (n=127)	Fragmentation composite (n=127)	Hypoxia composite (n=118)	Perfusion (n=124)	Metabolism (n=87)	Amyloid burden (n=125)	GM volume (n=127)
Mattis Dementia Rating Scale	r=.83	r=.06	r=.003	r=.02	r=.03	r=.07	r=-.10
	p=.38	p=.51	p=.98	p=.86	p=.78	p=.44	p=.30
Attention	r=.06	r=.07	r=.02	r=.16	r=-.01	r=.07	r=.06
	p=.54	p=.49	p=.80	p=.08	p=.91	p=.44	p=.529
Processing speed	r=-.02	r=.003	r=.03	r=.04	r=.05	r=.02	r=-.05
	p=.88	p=.98	p=.75	p=.66	p=.69	p=.84	p=.63
Working memory	r=-.01	r=-.03	r=-.005	r=-.007	r=.04	r=-.11	r=-.02
	p=.91	p=.76	p=.96	p=.94	p=.76	p=.22	p=.80
Executive functions	r=-.06	r=-.07	r=-.16	r=.08	r=.11	r=-.09	r=-.01
	p=.51	p=.45	p=.09	p=.41	p=.35	p=.34	p=.90
Episodic memory	r=-.09	r=-.12	r=-.17	r=-.05	r=-.08	r=-.19	r=-.12
	p=.35	p=.20	p=.08	p=.59	p=.50	p=.04	p=.21
Cognitive Difficulties Scale	r=.06	r=.04	r=.09	r=.07	r=-.03	r=-.06	r=.12
	p=.53	p=.69	p=.35	p=.47	p=.80	p=.52	p=.18
Pittsburgh Sleep Quality Index	r=.14	r=.03	r=-.03	r=.11	r=.07	r=.05	r=.22
	p=.14	p=.78	p=.73	p=.23	p=.55	p=.61	p=.02
Epworth sleepiness scale	r=-.04	r=-.03	r=-.03	r=.13	r=.08	r=.05	r=.06
	p=.69	p=.75	p=.76	p=.17	p=.49	p=.60	p=.52

Abbreviations: AHI, apnea-hypopnea index; ApoE, apolipoprotein E; GM, gray matter; SDB, sleep-disordered breathing.
Partial correlations were adjusted for age, sex, education, body mass index, sleep medication use and ApoE4 status. R values correspond to partial correlation coefficients, and results were considered significant at $p<0.0008$, after applying a Bonferroni correction for multiple testing ($p=0.05/63$).

eReferences.

1. Müller-Gärtner HW, Links JM, Prince JL, et al. Measurement of radiotracer concentration in brain gray matter using positron emission tomography: MRI-based correction for partial volume effects. *J Cereb Blood Flow Metab*. 1992;12(4):571-583. doi:10.1038/jcbfm.1992.81
2. La Joie R, Perrotin A, de La Sayette V, et al. Hippocampal subfield volumetry in mild cognitive impairment, Alzheimer's disease and semantic dementia. *NeuroImage Clin*. 2013;3:155-162. doi:10.1016/j.nicl.2013.08.007